energies

MDPI

Article

Impact of Hydrogen Injection on Natural Gas Measurement

Marco Dell'Isola [1,*], Giorgio Ficco [1], Linda Moretti [1], Jacek Jaworski [2], Paweł Kułaga [2] and Ewa Kukulska—Zając [2]

[1] Department of Civil and Mechanical Engineering, University of Cassino and South Lazio, 03043 Cassino, Italy; g.ficco@unicas.it (G.F.); linda.moretti@unicas.it (L.M.)
[2] Oil and Gas Institute—National Research Institute, ul. Lubicz 25a, 31-503 Kraków, Poland; jaworski@inig.pl (J.J.); pawel.kulaga@inig.pl (P.K.); ewa.kukulska@inig.pl (E.K.–Z.)
* Correspondence: dellisola@unicas.it

Abstract: Hydrogen is increasingly receiving a primary role as an energy vector in ensuring the achievement of the European decarbonization goals by 2050. In fact, Hydrogen could be produced also by electrolysis of water using renewable sources, such as photovoltaic and wind power, being able to perform the energy storage function, as well as through injection into natural gas infrastructures. However, hydrogen injection directly impacts thermodynamic properties of the gas itself, such as density, calorific value, Wobbe index, sound speed, etc. Consequently, this practice leads to changes in metrological behavior, especially in terms of volume and gas quality measurements. In this paper, the authors present an overview on the impact of hydrogen injection in natural gas measurements. In particular, the changes in thermodynamic properties of the gas mixtures with different H_2 contents have been evaluated and the effects on the accuracy of volume conversion at standard conditions have been investigated both on the theoretical point of view and experimentally. To this end, the authors present and discuss the effect of H_2 injection in gas networks on static ultrasonic domestic gas meters, both from a theoretical and an experimental point of view. Experimental tests demonstrated that ultrasonic gas meters are not significantly affected by H_2 injection up to about 10%.

Keywords: hydrogen; natural gas; gas meter; ultrasonic; thermal mass; gas chromatograph

Citation: Dell'Isola, M.; Ficco, G.; Moretti, L.; Jaworski, J.; Kułaga, P.; Kukulska–Zając, E. Impact of Hydrogen Injection on Natural Gas Measurement. *Energies* **2021**, *14*, 8461. https://doi.org/10.3390/en14248461

Academic Editor: Wei-Hsin Chen

Received: 8 November 2021
Accepted: 8 December 2021
Published: 15 December 2021

1. Introduction

In 2020, the European Commission (EC) published the European Union (EU) hydrogen strategy on the roadmap to develop an integrated energy system based on the large-scale hydrogen supply chain [1]. The EU hydrogen strategy has the twofold objective of expanding hydrogen use to replace fossil fuels and to decarbonize its production. In detail, the path set by the EC is divided into three phases. The first phase entails the installation of at least 6 GW of renewable hydrogen electrolysers in the EU by 2024 and producing up to one million tonnes of renewable hydrogen. The second one relies on the installation of at least another 40 GW of renewable hydrogen electrolysers by 2030 and the production of up to 10 million tons of renewable hydrogen in the EU. The third and last phase aims to deploy large scale renewable hydrogen technologies to reach all hard-to-decarbonise sectors by 2050.

To achieve such goals, it will be effective to consider the reuse of the existing natural gas (NG) infrastructure. The latter will play a crucial role in the development of a decarbonized energy system based on a large usage of hydrogen as energy carrier due to its widespread presence and its capacity to provide a cost-effective option for transporting and storing large amounts of energy for long-term periods, exploiting the NG transportation and distribution networks, as well as the storage complexes of the existing NG infrastructure.

On the other hand, the increasing weight of the non-programmable renewable energy sources (RES), such as photovoltaic and wind in power generation, is currently leading

to relevant issues on the management of the electricity grid, owing to their intermittent and random nature. Indeed, power production from non-programmable RES does not follow the dynamics of energy consumption, generating critical supply–demand issues, specifically in overgeneration periods. The storage capacities required to guarantee the stability and flexibility of the electrical energy system can be ensured by the application of power to gas technologies [2]. In fact, the hydrogen produced from RES during overgeneration periods can be injected into NG pipelines, thus overcoming balancing and regulation issues related to the electricity grid management, as well as decarbonizing end use sectors (e.g., residential, urban and public transport, industrial).

Thus, the blending of hydrogen produced from RESs into NG mixtures nowadays represents an effective tool for developing a climate neutral integrated energy system. Nevertheless, several factors must be considered to assess the possibility of using mixtures of hydrogen and natural gas (H2NG) into existing network components (e.g., pipelines, valves, compressor, measuring systems). In fact, increasing content of hydrogen lead to significant changes in physical and thermal properties of the flowing gaseous mixture.

The changes in thermodynamic properties, in turn, result in changes in ignition and energy properties. In particular, hydrogen enrichment strongly induces non-linear effects in terms of burning velocity, interaction of the propagating flame with the turbulent flow field and, consequently, explosion behaviour [3]. The major risk associated with hydrogen is the possibility of having explosive atmosphere conditions, which has been demonstrated by numerous studies on explosive characteristics dust and gas hydrides [4]. As a consequence, hydrogen is more hazardous and more susceptible to deflagration-to-detonation transition than hydrocarbons. Therefore, the addition of hydrogen could pose minor or major safety issues depending on the volumetric percentage of hydrogen added (e.g., fugitive emissions are larger with hydrogen, flammability limits of hydrogen are wider than methane) [5]. In general, few minor issues occur with blends of hydrogen content ranging up to 5–15% in volume, depending on site specific conditions and particular NG compositions. Therefore, it is agreed that extensive studies and tests of pipelines, compressor, valves, measuring devices and appliances are needed [6].

Several studies have been devoted to the analysis of the effects of H_2 injection on the measuring devices' reliability. In [7], the changes in the properties of different gas belonging to the "H" group of EN 437:2019 were investigated, demonstrating that all gases still remain classified as "H" group when a content of H_2 in the range from 2% to 23% is injected in the gas itself. In particular, the physical and thermal properties of the mixtures change as follows: (i) the speed of sound increases in the range 1–13.5%; (ii) the relative density reduces by 1.7–20.5%; (iii) the higher calorific value reduces by 1.4–16%; (iv) the Wobbe index reduces by 0.49–5.7%. In conclusion, it is affirmed no particular substitution of components, nor modifications in the algorithms for calculating physical parameters of the gas mixture and volumetric flow (volume) are needed when about 10% hydrogen is injected into natural gas, allowing for maintaining substantially unaltered existing management practices in gas transportation and consumption systems. Conversely, further investigations are suggested in the case of higher H_2 contents. Similarly, with H_2 injection up to 30% no particular problems for construction materials of ultrasonic, volumetric diaphragm and turbine gas meters are expected [8]. However, experimental tests aimed at assessing gas meters in terms of measurement accuracy and long-term reliability are suggested. Iskov [9] analysed the impact of 100% hydrogen after one-year operation of traditional turbine, volumetric rotary piston and diaphragm gas meters in a distribution network configuration (i.e., at a pressure of 20 mbar), demonstrating H_2 does not affect the accuracy of such gas meters, despite some issues with the turbine meter seal. Dehaeseleer [10] found no operational issues for traditional gas meters (turbine, rotary piston and diaphragm) up to 10% of H_2. The durability of diaphragm gas meters has been evaluated by Jaworski [11] with H2NG and no significant influence has been found with H_2 up to 15%. Jaworski and Dudek [12] investigated domestic thermal gas meters, demonstrating that they do not exceed maximum permitted errors (MPE) with 2, 4 and 5%

of H_2 content. Conversely, with increasing H2 content of 10 and 15% they systematically showed negative drifts of the errors (e.g., up to −3.4% and −8.4% of the weighted mean error (WME), at 10% and 15% of H_2, respectively).

Experimental studies in the literature for ultrasonic meters are not available, and experimental research for H_2 content above 10% is suggested on the kind of meters in [13]. Finally, Łach [14] investigated the issues of H_2 injection on the compressibility factor, which is critical for the volume conversion at standard conditions. To this aim, tests were carried out to compare SGERG-88 and AGA8-DC92 algorithms with increasing H_2 contents, due to the fact that both algorithms present the application limit of H_2 = 10% (mol/mol). The experimental results demonstrated that the AGA8-DC92 algorithm provides satisfactory results with H_2 content below 40% (mol/mol).

This paper presents an overview on the effect of hydrogen injection in natural gas measurements. With the aim of assessing the reliability of measuring devices that currently run on the existing NG infrastructures, the authors analysed the effect of hydrogen injection on gas measurements, both from a theoretical and an experimental point of view. In detail, a comprehensive analysis of the changes of thermo-physical properties when gases with different H_2 content are used has been carried out, as well as of the theoretical effects on the accuracy of volume conversion at standard conditions. The impact of the hydrogen injection on the accuracy of static ultrasonic domestic gas meters has also been experimentally investigated for the first time to the best knowledge of the authors, and the related results have been presented and discussed.

2. Theory and Methods

2.1. Thermodynamic Properties

According to the ISO 6976:2017 [15], the density $D^0(p,\ t)$ of an ideal gas depends upon its temperature t and pressure p and shall be calculated from Equation (1). Consequently the density $D(p,\ t)$ of a real gas is obtained through Equation (2) where: (i) $Z(p,t)$ is the compressibility factor of the gaseous mixture [16]; (ii) V^0 is the ideal molar volume evaluated according to the ideal gas law; (iii) M is the molar mass of the gas mixture calculated through Equation (3), in which x_j is the mole fraction of the j-th component in the gas mixture and M_j is the molar mass of the j-th component.

$$D^0(p,\ t) = \frac{M}{V^0} \tag{1}$$

$$D(p,\ t) = \frac{D^0}{Z(p,t)} \tag{2}$$

$$M = \sum_{j=1}^{N} x_j M_j \tag{3}$$

The relative density $G(p,t)$ of a real gas mixture is given by the ratio of the density of the gaseous mixture to the density of dry air of reference composition at the same pressure and temperature conditions. Therefore, according to [15], $G(p,t)$ can be calculated through Equation (4) where: (i) $Z_{air}(p,t)$ is the compressibility factor of dry air, (ii) $Z(p,t)$ is the compressibility factor of the gas, and (iii) G^0 is the relative density of the ideal gas calculated through Equation (5). In Equation (5) x_j and M_j respectively represent the mole fraction and the molar mass of the j-th component, whereas M_{air} is the molar mass of dry air of reference composition.

$$G(p,t) = \frac{G^0 \cdot Z_{air}(p,t)}{Z(p,t)} \tag{4}$$

$$G^0 = \sum_{j=1}^{N} x_j \frac{M_j}{M_{air}} \tag{5}$$

The specific heat capacity at constant pressure $c_p(t)$ is obtained through the weighted average of the specific heat capacities at constant pressure $c_{p,j}$ of the j-th components, in which mass fraction is x_j For the calculation of $c_{p,j}$ the following Equation (7) can be used, where T is the absolute temperature and A_j, B_j, C_j, D_j, E_j are the regression coefficients for the j-th component reported in Table 1.

$$c_p(t) = \sum_{j=1}^{N} x_j \cdot c_{p,j} \tag{6}$$

$$c_{p,j}(T) = A_j + B_j\, T + C_j\, T^2 + D_j\, T^3 + E_j\, T^4 \tag{7}$$

Table 1. Regression coefficients of gas components [16].

Component, *j*	Temperature Range [K]	A	B	C	D	E
Methane, CH_4	50–1500	34.942	$-3.9957\ 10^{-2}$	$1.9184\ 10^{-4}$	$-1.5303\ 10^{-7}$	$3.9321\ 10^{-11}$
Ethane, C_2H_6	100–1500	28.146	$4.3447\ 10^{-2}$	$1.8946\ 10^{-4}$	$-1.9082\ 10^{-7}$	$5.3349\ 10^{-11}$
Propane, C_3H_8	200–1000	31.986	$4.27\ 10^{-2}$	$5.00\ 10^{-4}$	$-6.56\ 10^{-7}$	$2.56\ 10^{-10}$
n-Butane, n-C_4H_{10}	200–1500	20.056	$2.8153\ 10^{-1}$	$-1.3143\ 10^{-5}$	$-9.4571\ 10^{-8}$	$3.4149\ 10^{-11}$
iso-Butane, iso-C_4H_{10}	200–1500	6.772	$3.1447\ 10^{-1}$	$-1.0271\ 10^{-4}$	$-3.6849\ 10^{-8}$	$2.0429\ 10^{-11}$
n-Pentane, n-C_5H_{12}	200–1500	26.671	$3.2324\ 10^{-1}$	$4.2820\ 10^{-5}$	$-1.6639\ 10^{-7}$	$5.6036\ 10^{-11}$
iso-Pentane, iso-C_5H_{12}	200–1000	16.288	$3.1754\ 10^{-1}$	$2.0237\ 10^{-4}$	$-4.3027\ 10^{-7}$	$1.8001\ 10^{-11}$
n-Hexane, C_6H_{14}	200–1500	25.924	$4.1927\ 10^{-1}$	$-1.2491\ 10^{-5}$	$-1.5592\ 10^{-7}$	$5.8784\ 10^{-11}$
Nitrogen, N_2	50–1500	29.342	$-3.5395\ 10^{-1}$	$1.0076\ 10^{-5}$	$-4.3116\ 10^{-9}$	$2.5935\ 10^{-13}$
Carbon dioxide, CO_2	50–5000	27.437	$4.2315\ 10^{-2}$	$-1.9555\ 10^{-5}$	$3.9968\ 10^{-9}$	$-2.9872\ 10^{-13}$
Hydrogen, H_2	250–1500	25.399	$2.0178\ 10^{-2}$	$-3.8549\ 10^{-5}$	$3.1880\ 10^{-8}$	$-8.7585\ 10^{-12}$

The higher calorific value $(Hv)_G^0$ at a given temperature t, is calculated through Equation (8) in which $(Hv)_G^0(t)$ is the ideal higher molar-basis calorific value and V^0 is the ideal molar volume of the mixture calculated according to the ideal gas law.

$$(Hv)_G^0(p,t) = \frac{(Hc)_G^0(t)}{V^0} \tag{8}$$

The Wobbe index is the ratio of the higher calorific value, at specified reference condition, to the square root of the relative density and it is given by Equation (9) where $(Hv)_G^0$ is the higher calorific value on volume basis and G^0 is the relative density of the gas.

$$W_G^0(t,p) = \frac{(Hv)_G^0(t,p)}{\sqrt{G^0}} \tag{9}$$

Finally, the speed of sound in a gaseous flow can be obtained through Equation (10) using the AGA 10 Equation [17]

$$u = 18.591 \left(\frac{T \cdot Z \cdot k}{D} \right)^{0.5} \tag{10}$$

2.2. Volume Conversion Factor

The accurate knowledge of NG volumetric flow rate is crucial in commercial transactions and balancing issues of the NG infrastructures. To this aim, the NG mixture volume measured at operative conditions is commonly converted to the standard reference conditions (i.e., p_S = 101,325 kPa, T_S = 15 °C). Such volume conversion is obtained through

Equation (11) where: (i) V_s and V are the NG mixture volume at reference and metering conditions, respectively; (ii) $KTvo$ is the volumetric correction factor.

$$V_S = V \cdot KTvo = V \cdot \frac{p}{p_S} \cdot \frac{T_S}{T} \cdot \frac{Z_S}{Z} \tag{11}$$

In Equation (11) the following symbols have been used: (i) p_S and p are the absolute pressure at reference and metering conditions, respectively; (ii) T_S and T are the temperature at reference and metering conditions, respectively; (iii) Z_S and Z are the compressibility factor calculated at reference and metering conditions, respectively.

According to [15] the comprsibility factor at reference conditions Z_S is calculated through Equation (12) where: (i) $p_0 = 101,325$ kPa is the reference pressure and p_2 is the pressure at metering conditions; (ii) x_j is the mole fraction of the j-th component in the gas mixture; (iii) s_j is the summation factor of the j-th component in the gas mixture, whose values are reported in [15] at the metering reference temperatures.

$$Z_S = 1 - \left(\frac{p}{p_0}\right) \cdot \left[\sum_{j=1}^{n} x_j \cdot s_j(t,p)\right]^2 \tag{12}$$

On the other hand, the compressibility factor at metering conditions, Z, has been calculated according to the ISO 12213–2:2010 standard [18]. The standard employs the AGA8-DC92 detailed characterization equation in [19], which is an extended virial-type formulation, only capable of calculating the properties in the gaseous phase. The input data are the absolute pressure, absolute temperature and the detailed molar-composition of the gas, as detailed in Equation (13) where: (i) B is the second virial coefficient; (ii) ρ_m is the molar density; (iii) ρ_r is the reduced density; (iv) b_n, c_n, k_n are constants; (v) C_n^* are the coefficients, which depend on the temperature, and NG mixture composition.

$$Z = 1 + B\rho_m - \rho_r \sum_{n=13}^{18} C_n^* + \sum_{n=13}^{58} C_n^* \left(b_n - c_n k_n \rho_r^{k_n}\right) \rho_r^{k_n} exp\left(-c_n \rho_r^{k_n}\right) \tag{13}$$

The reduced density ρ_r is correlated to the molar density ρ_m through Equation (14) where K is a mixture size coefficient and ρ_m is the molar density calculated using Equation (15) in which p and T respectively represent the absolute pressure and temperature and R is the universal gas constant.

$$\rho_r = K^3 \rho_m \tag{14}$$

$$\rho_m = \frac{p}{ZRT} \tag{15}$$

By observing Equation (11), it can be pointed out the NG volume at base condition is highly influenced by the compressibility factor. Therefore, the algorithm used for the calculation of the compressibility factor is a crucial issue especially for large flow metering systems in NG industries applications [20]. In order to assess its reliability, the authors carried out the calculation of the compressibility factor through the currently available algorithms ISO 12213-3, AGA NX 19 and AGA NX 19 Mod.

2.3. Ultrasonic Static Gas Meter Measuring Principles

The ultrasonic gas meters for domestic use determine the volume of the gas flowing through the gas meter measuring the transit times (e.g., time of flight, TOF) of the ultrasonic waves generated by a pair of piezoelectric transducers operating as transmitter/receiver (see Figure 1). The measurement of the transit times (e.g., t_1 and t_2) and the knowledge of geometric characteristics of the measurement tube (e.g., diameter, D_t, propagation angle, φ and distance between the two transducers, L) allows one to calculate the average velocity

($\overline{w}$) of the gas flow and, therefore, the volumetric flow rate (Q), employing the following equation:

$$\overline{w} = \frac{L}{2\,cos\varphi}\left(\frac{1}{t_1} - \frac{1}{t_2}\right) = \frac{L^2}{2\,D}\cdot\frac{\Delta t}{t_1\,t_2} = \frac{L^2}{2\,D}\cdot\Delta f \tag{16}$$

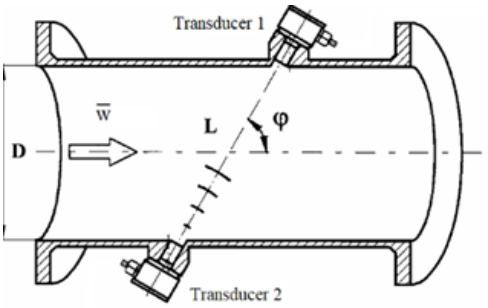

Figure 1. Measurement principle of the ultrasonic gas meters.

Since the sound of speed in the gas flow (u) is unknown, depending on the thermodynamic state (e.g., pressure and temperature) and composition of the fluid, the measurement of $\overline{w}$ is performed thorough the measurement of transit times of two different ultrasonic signals. The transit time (t_1) of an ultrasonic signal traveling cocurrent with the gas flow from Transducer 1 to Transducer 2 is measured. After the measurement is completed, the transit time (t_2) of an ultrasonic signal traveling counter current to the gas flow from Transducer 2 to Transducer 1 is measured. Specifically, the transit time of the signal cocurrent with the gas flow will be lower than that of the signal counter current with the gas flow, owing to the velocity of the gas within the meter. This involves different frequencies of the two train waves.

From the analysis of Equation (16), it can be deduced that the average velocity ($\overline{w}$), and consequently the volumetric flow rate (Q), is not theoretically influenced by the thermodynamic conditions and composition of the gas flow. However, if the speed of sound is analysed it can be observed that it is significantly influenced by the H_2 content in the NG mixture.

The effects of gas mixtures of variable compositions (mixtures of natural gas, natural gas with hydrogen additives, and mixtures of synthetic biogas) on the accuracy of domestic gas meters (e.g., ultrasonic, thermal-mass and turbine) have been investigated widely [21] in the literature and recently at laboratories of the INiG-PIB [12]. To this aim, a test bench capable of testing the metrological performance of gas meters with natural gas mixtures with different H_2 content was designed and built, enabling measurement in the range of 0.016 to 25 m^3/h at low gas pressure (approx. 20 mbar). A wet drum gas meter (for flow-rate range up to 0.4 m^3/h) and a rotary gas meter (in the range from 0.3 to 25 m^3/h) were used as reference gas meters. The measurement uncertainty on the test bench is within 0.3% in the range from 0.6 to 6 m^3/h and within 0.45% below 0.6 m^3/h. The research program included testing the errors of indications with the use of the gas mixtures presented in Table 2.

Table 2. Characteristics of the gas mixtures used for the metrological tests.

Sample	Gas Mixture
Air	Atmospheric air
2E/H0	2E natural gas mixture, without hydrogen
2E/H5	2E natural gas mixture, with 5% hydrogen content (V/V)
2E/H10	2E natural gas mixture, with 10% hydrogen content (V/V)

3. Results and Discussion

3.1. Impact of H_2 Injection on the Thermodynamic Properties

In order to analyse the impacts of hydrogen injection in NG mixtures on the above mentioned thermodynamic properties, the five NG mixtures in Table 3 have been investigated (i.e., the ones in [18] without H_2) and the obtained results have been graphically represented in Figure 2.

Table 3. Investigated gas mixtures [18].

Component, *j*	Mix 1	Mix 2	Mix 3	Mix 5	Mix 6
Methane, CH_4	96.50	90.70	85.90	81.20	82.60
Ethane, C_2H_6	1.80	4.50	8.50	4.30	3.50
Propane, C_3H_8	0.45	0.84	2.30	0.90	0.75
n-Butane, n-C_4H_{10}	0.10	0.15	0.35	0.15	0.12
iso-Butane, iso-C_4H_{10}	0.10	0.10	0.35	0.15	0.12
n-Pentane, n-C_5H_{12}	0.03	0.04	0.05	0.00	0.04
iso-Pentane, iso-C_5H_{12}	0.05	0.03	0.05	0.00	0.04
n-Hexane, C_6H_{14}	0.07	0.04	0.00	0.00	0.02
Nitrogen, N_2	0.30	3.10	1.00	5.70	11.70
Carbon dioxide, CO_2	0.60	0.50	1.50	7.60	1.10

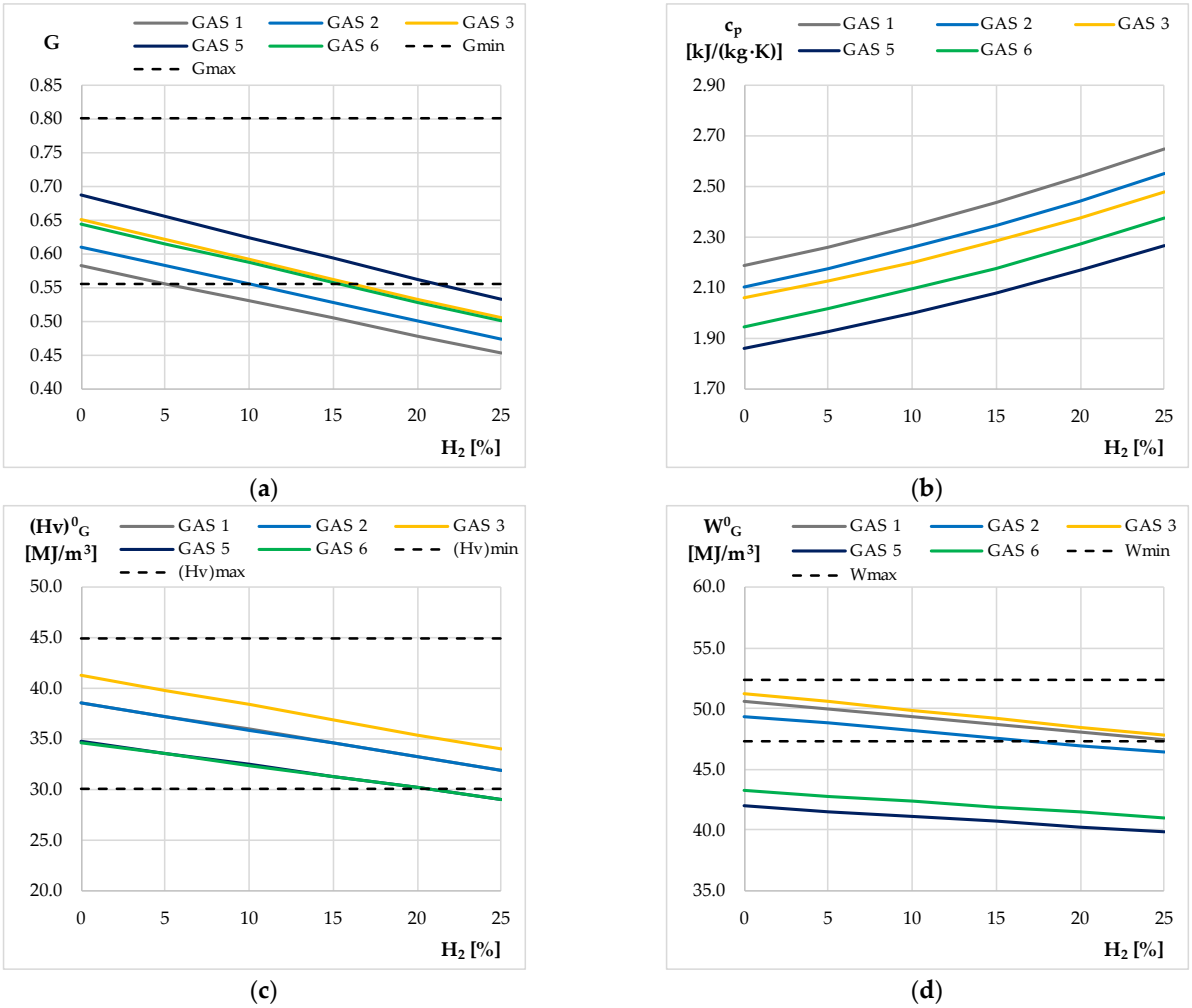

Figure 2. Trend of the thermophysical properties as a function of the H_2 content in NG mixtures: (**a**) relative density, (**b**) specific heat capacity, (**c**) higher calorific value, (**d**) Wobbe Index. Dashed lines represent the applicable limits [18,22].

In Figure 3, the trend of the sound speed as a function of the H_2 content for the 5 NG mixture reported in Table 1 has been depicted. From Figure 3 it can be pointed out the speed of sound increases as H_2 concentration in the NG mixture increases and it exceeds the allowable limit of 475 m·s^{-1}, in some cases even at low H_2 content.

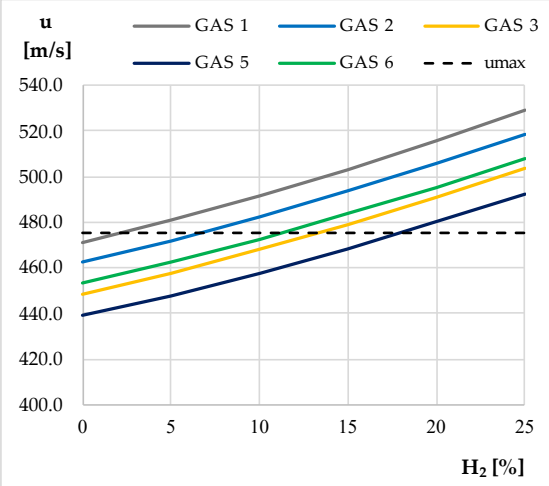

Figure 3. Trend of the sound speed as a function of the H_2 content in NG mixtures. Dashed line represents the applicable limit [23].

Hence, even though the measurement of the gas flow velocity is not theoretically influenced by the speed of sound, since this is intrinsically compensated by the sing-around technique and mediated in the cross section (no effect in the transition of the flow from laminar to turbulent), the change of transit times measured in favor and against flow can lead to unpredictable deviations and a drift in the accuracy of the gas meters.

From the analysis of the obtained results, it can be highlighted that:

- the relative density decreases as the H_2 content increases in the NG mixture leading to values below the corresponding limit of ISO 12213-2 standard [18] at about 10% of H_2;
- the specific heat capacity at constant pressure significantly increases as the H_2 content increases (e.g., up to +21.8% at about 25% of H_2 for Gas 6);
- the higher calorific value on volume basis notably decreases as the H_2 content increases (e.g., up to −17.8% for Gas 3 at x_{H_2} = 25%) and for investigated Gas 5 and 6, it reduces to below the corresponding limit indicated by the ISO 12213-2 standard [18] at about 25% of H_2;
- the Wobbe index slightly decreases as the H_2 content increases (e.g., up to −6.6% at x_{H_2} = 25% for Gas 2);
- the speed of sound increases as the H_2 content increases.

3.2. Impact of H_2 Injection on the Volume Conversion

In order to evaluate the effects of injection of H_2 in NG mixtures on the accuracy of the volume conversion at standard conditions, a typical NG mixture distributed in Italy has been investigated (see Table 4).

Table 4. Molar composition of the investigated gas mixture.

Component, *j*	MIX 4
Methane, CH_4	95.99
Ethane, C_2H_6	2.292
Propane, C_3H_8	0.639
n-Butane, n-C_4H_{10}	0.097
iso-Butane, iso-C_4H_{10}	0.102
n-Pentane, n-C_5H_{12}	0.012
iso-Pentane, iso-C_5H_{12}	0.018
n-Hexane, C_6H_{14}	0.012
Nitrogen, N_2	0.650
Carbon dioxide, CO_2	0.188

Figure 4 depicts the effects of the increase of H_2 content up to 25% in the investigated NG mixture on the compressibility factor calculated employing the aforementioned standards. Moreover, to investigate the influence of the metering pressure, the compressibility factor calculation has been performed at different gas pressures fixing a constant value of the gas temperature (i.e., T = 15 °C).

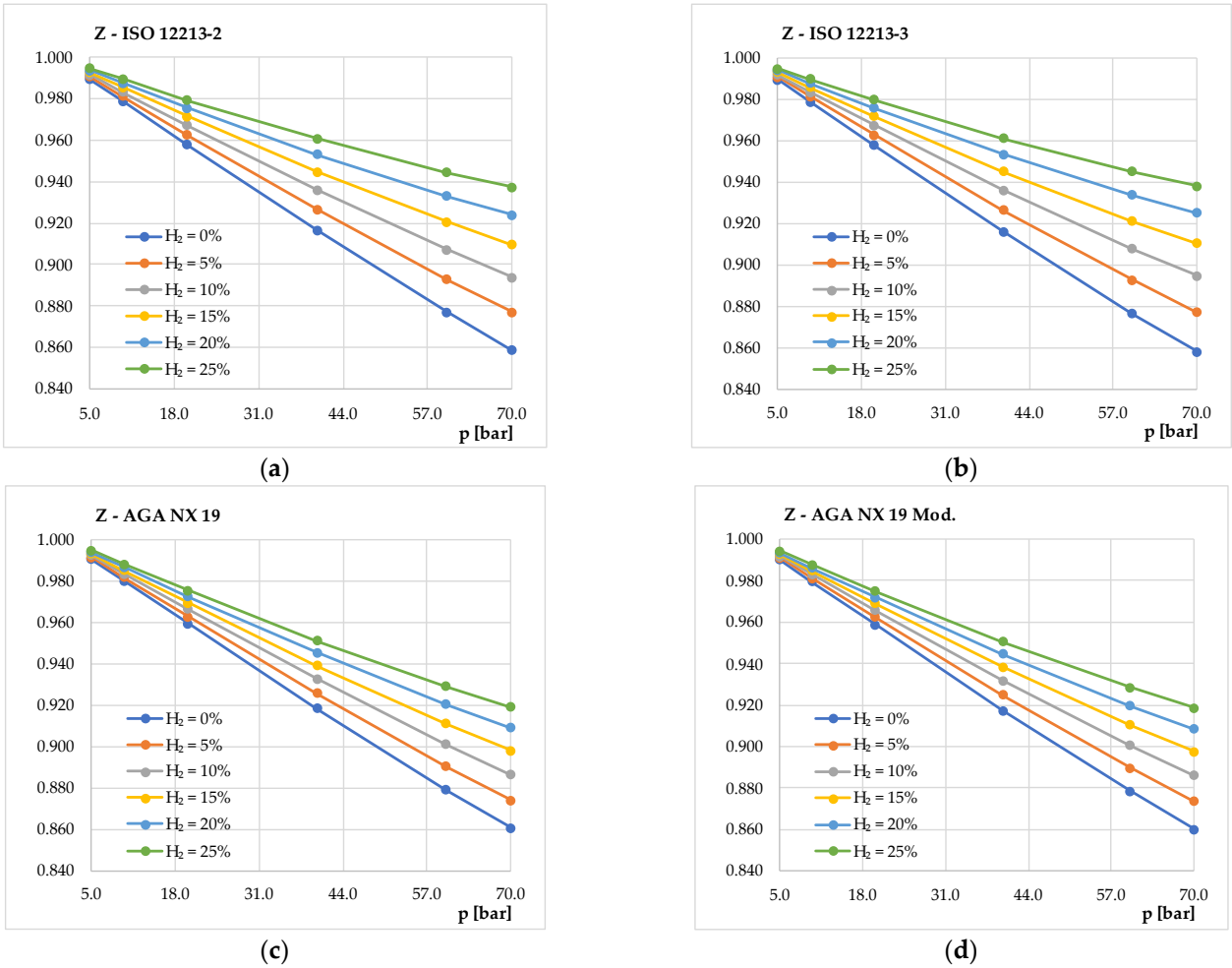

Figure 4. Trend of the compressibility factor in NG and H_2 mixtures: (**a**) ISO 12213-2, (**b**) ISO 12213-3, (**c**) AGA NX 19 and (**d**) AGA NX 19 Mod.

From data in Figure 4, it can be pointed out that the compressibility factor increases as the H_2 content increases. The compressibility factor is more influenced by the H_2 concentration at high pressures than at low pressures. As, for example, *Z* increases in the range

0.10–0.44% at 5 bar and 2.1–9.1% at 70 bar when ISO 12213-2 standard is used. Moreover, pressure more significantly affects the compressibility factor at low H_2 concentrations and, as expected, *Z* decreases as pressure increases (e.g., Z decreases in the range 0.25–14% at x_{H_2} = 0%, whereas a lower decrease in the range 0.05–0.2% at x_{H_2} = 25% occurs).

In Table 5, the compressibility factor values and the corresponding deviations between the ISO 12213-2 standard and the other standards on varying the H_2 concentration and pressure have been reported. From data in Table 5 it can be observed that ISO 12213-2 and ISO 12213-3 methods lead to deviations within 0.09%, whereas the use of AGA NX 19 and AGA NX 19 Mod. methods can lead to deviations up to about 2% at high pressure and high H_2 content.

Table 5. Compressibility factor values evaluated employing the ISO 12213-2, ISO 12213-3, AGA NX 19 and AGA NX 19 Mod.

p [bar]	H_2 [%]	$Z_{ISO12213-2}$	$Z_{ISO12213-3}$	$Z_{AGANX19}$	$Z_{AGANX19Mod}$	$\Delta Z_{ISO2-ISO3}$	$\Delta Z_{ISO2-AGA19}$	$\Delta Z_{ISO2-AGA19Mod.}$
5.00	0.00	0.98940	0.99026	0.99026	0.98997	0.09%	0.09%	0.06%
	0.50	0.99056	0.99118	0.99118	0.99090	0.06%	0.06%	0.03%
	10.00	0.99167	0.99206	0.99206	0.99179	0.04%	0.04%	0.01%
	15.00	0.99273	0.99290	0.99290	0.99262	0.02%	0.02%	0.01%
	20.00	0.99374	0.99369	0.99369	0.99342	0.00%	0.00%	0.03%
	25.00	0.99469	0.99445	0.99445	0.99417	0.02%	0.02%	0.05%
10.00	0.00	0.97881	0.97868	0.97974	0.97943	0.01%	0.09%	0.06%
	0.50	0.98117	0.98108	0.98154	0.98124	0.01%	0.04%	0.01%
	10.00	0.98341	0.98337	0.98326	0.98296	0.00%	0.02%	0.05%
	15.00	0.98555	0.98553	0.98489	0.98460	0.00%	0.07%	0.10%
	20.00	0.98757	0.98756	0.98643	0.98614	0.00%	0.12%	0.14%
	25.00	0.98949	0.98948	0.98789	0.98760	0.00%	0.16%	0.19%
20.00	0.00	0.95774	0.95748	0.95906	0.95871	0.03%	0.14%	0.10%
	0.50	0.96256	0.96243	0.96266	0.96232	0.01%	0.01%	0.03%
	10.00	0.96713	0.96709	0.96607	0.96574	0.00%	0.11%	0.14%
	15.00	0.97146	0.97147	0.96930	0.96897	0.00%	0.22%	0.26%
	20.00	0.97555	0.97558	0.97234	0.97202	0.00%	0.33%	0.36%
	25.00	0.97941	0.97944	0.97522	0.97491	0.00%	0.43%	0.46%
40.00	0.00	0.91635	0.91588	0.91803	0.91734	0.05%	0.18%	0.11%
	0.50	0.92642	0.92629	0.92545	0.92480	0.01%	0.11%	0.17%
	10.00	0.93586	0.93595	0.93242	0.93182	0.01%	0.37%	0.43%
	15.00	0.94471	0.94492	0.93898	0.93841	0.02%	0.61%	0.67%
	20.00	0.95300	0.95324	0.94515	0.94461	0.02%	0.82%	0.88%
	25.00	0.96076	0.96094	0.95094	0.95044	0.02%	1.02%	1.07%
60.00	0.00	0.87694	0.87628	0.87880	0.87825	0.07%	0.21%	0.15%
	0.50	0.89254	0.89255	0.89020	0.88968	0.00%	0.26%	0.32%
	10.00	0.90700	0.90741	0.90085	0.90036	0.04%	0.68%	0.73%
	15.00	0.92043	0.92101	0.91080	0.91033	0.06%	1.05%	1.10%
	20.00	0.93290	0.93349	0.92011	0.91966	0.06%	1.37%	1.42%
	25.00	0.94448	0.94493	0.92881	0.92839	0.05%	1.66%	1.70%
70.00	0.00	0.85843	0.85769	0.86052	0.85992	0.09%	0.24%	0.17%
	0.50	0.87682	0.87695	0.87387	0.87331	0.02%	0.34%	0.40%
	10.00	0.89378	0.89441	0.88631	0.88578	0.07%	0.84%	0.89%
	15.00	0.90945	0.91028	0.89791	0.89742	0.09%	1.27%	1.32%
	20.00	0.92394	0.92475	0.90874	0.90827	0.09%	1.65%	1.70%
	25.00	0.93736	0.93797	0.91883	0.91839	0.07%	1.98%	2.02%

Finally, the authors investigated the effects of H_2 injection on the volumetric correction factor, *KTvo*. From Figure 5, it can be pointed out that the volumetric correction factor decreases as the H_2 content increases, regardless of the calculation algorithm used. Similarly to the compressibility factor, the H_2 content affects *KTvo* more at high pressures than at low pressures. As for example, the *KTvo* calculated with the ISO 12213-2 standard decreases as H_2 increase by 0.10–0.43% at 5 bar, whereas it increases by 2.1–8.3% at 70 bar.

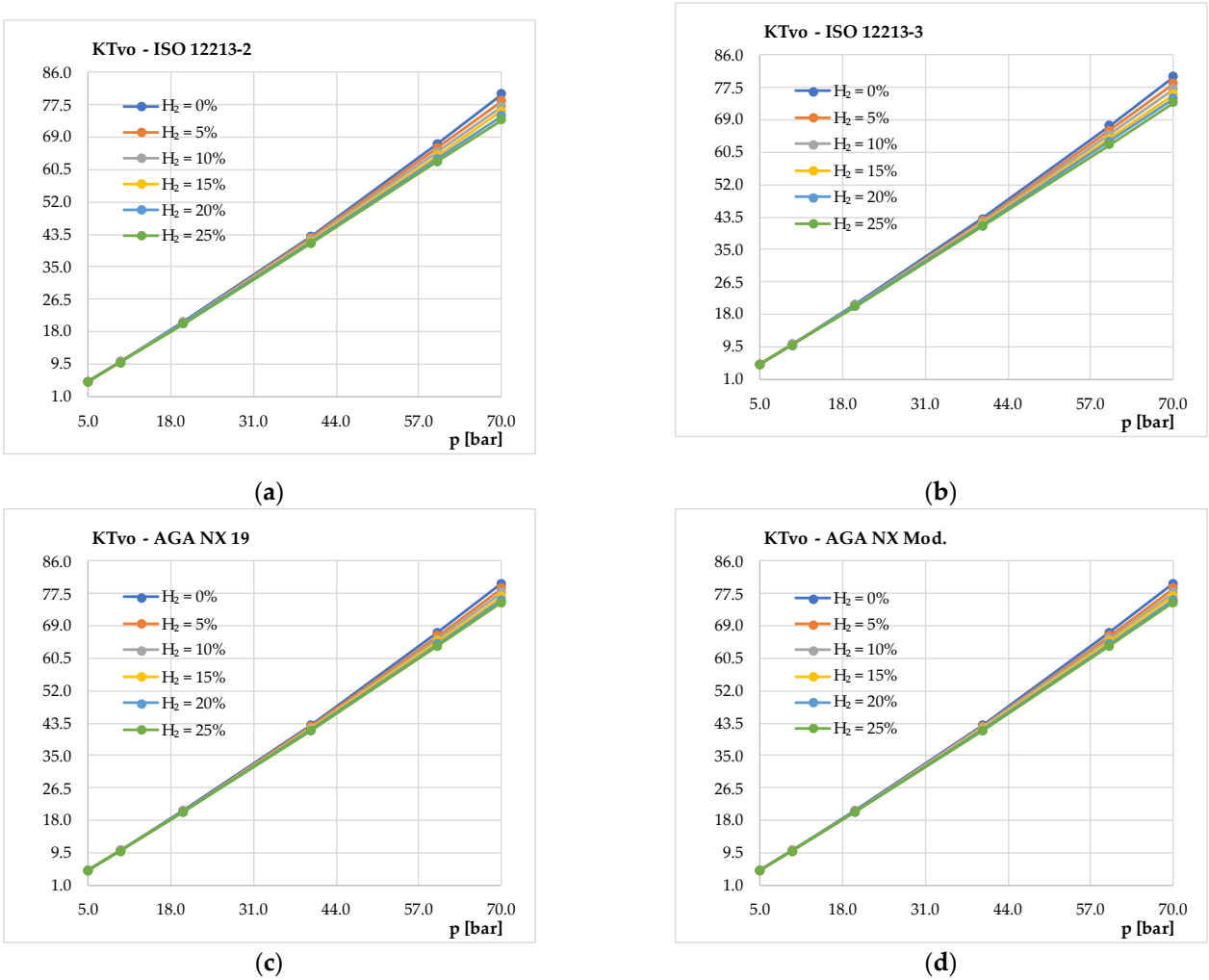

Figure 5. Trend of the volumetric correction factor in NG and H_2 mixtures: (**a**) ISO 12213-2, (**b**) ISO 12213-3, (**c**) AGA NX 19 and (**d**) AGA NX 19 Mod.

3.3. Impact of H2 Injection on Ultrasonic Domestic Gas Meters

Domestic ultrasonic gas meters manufactured in 2021, with a measuring range of 0.04 to 6 m^3/h, were subjected to metrological tests with the use of various gas mixtures. Metrological tests were carried out according to par. 5.3.2 of EN 14236:2018, at selected flow rates (Q_{min}, 3 Q_{min}, 0.1 Q_{max}, 0.2 Q_{max}, 0.4 Q_{max}, 0.7 Q_{max}, Q_{max}), each repeated three times. The gas mixtures listed in Table 2 have been used. Experimental test results are presented in Table 6 and Figure 6.

Table 6. Average errors and average errors of indication drifts as well as *WME*s and *WME*s drifts of G4 ultrasonic gas meters tested with different gas mixtures.

	Flow Rate							
	Q_{min}	**3 Q_{min}**	**0.1 Q_{max}**	**0.2 Q_{max}**	**0.4 Q_{max}**	**0.7 Q_{max}**	**Q_{max}**	
	Average error E_m [%]							*WME* [%]
E_{mAir}	−0.63	−0.99	−0.66	−0.44	−0.40	−0.11	−0.33	−0.30
$E_{m2E/H0}$	−0.81	−1.14	−0.32	−0.25	0.08	0.32	−0.06	0.07
$E_{m2E/H5}$	−0.10	−0.25	0.03	−0.26	−0.13	0.03	−0.49	−0.15
$E_{m2E/H10}$	−0.47	−0.65	0.14	−0.25	−0.28	−0.11	−0.53	−0.25
	Average error drift ΔE_m [%]							*WME* drift [%]
$\Delta E_{m2E/H5}$	0.71	0.88	0.35	−0.01	−0.21	−0.29	−0.43	−0.22
$\Delta E_{m2E/H10}$	0.34	0.48	0.46	0.00	−0.36	−0.43	−0.47	−0.31

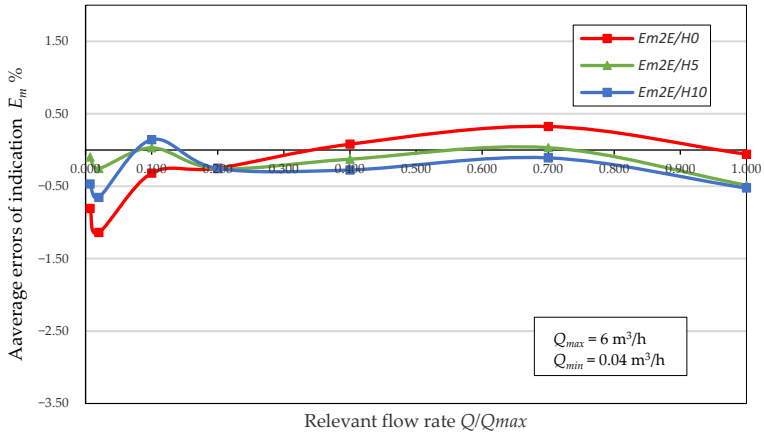

Figure 6. Average errors of indications of G4 ultrasonic gas meters tested with different gas mixtures as a function of relative flow rates Q/Q_{max}.

The average errors of indication of ultrasonic gas meters, the differences between the errors of indication obtained for reference natural gas and individual gas mixtures, and the metrological analysis of the obtained test results are presented below. For the metrological assessment, average error values were used, while, when analysing the maximum and minimum error values, the values obtained for each gas meter were used individually. In order to define the metrological criterion necessary to assess the impact of H_2 injection on the gas meter errors of indications (metrologically significant or metrologically insignificant), the measurement uncertainty at single flow rates was estimated. As the assessment covers the difference in the average errors of indications for individual mixtures in relation to the errors of indications obtained for the reference mixture of natural gas without hydrogen addition (e.g., between 2E/H0 and 2E/H5), the measurement uncertainty is the total uncertainty in determining the errors in gas meter readings for the gas reference 2E/H0 and the tested mixture with the addition of hydrogen or biogas (e.g., 2E/H5, 2E/H10). The uncertainty of the average errors of indications, $U(E_m)$, includes the type B uncertainty of the measuring equipment and the type A uncertainty (i.e., the standard deviation of the results of the three tested gas meters). The maximum allowable difference in errors $U(E_{mH\text{-}m2E})$ is obtained by the square sum $U(E_m)$ of the two mixtures; thus, the metrological assessment means "insignificant" if the difference in average errors is below the permitted errors difference.

In addition, the weighted mean errors (WME) was also evaluated according to par. 3.2.5 OIML R 137 1 & 2:2012 [24], according to which the WME for class 1.5 gas meters should be within ±0.6%. Table 6 shows the average errors of indications (E_{mAIR}, $E_{m2E/H0}$, $E_{m2E/H5}$, $E_{m2E/H10}$) obtained for individual gas mixtures, average differences ($\Delta E_{2E/H5}$, $\Delta E_{2E/H10}$) between the errors obtained for natural gas ($E_{m2E/H0}$) and individual gas mixtures ($E_{m2E/H5}$, $E_{m2E/H10}$), and weighted mean errors WMEs together with WMEs drift for G4 ultrasonic gas meters.

Figure 6 shows the average errors of indications of G4 ultrasonic gas meters obtained for the gas mixtures 2E/H0, 2E/H5, 2E/H10.

The error of indication of the investigated ultrasonic gas meters with 2E/H0 natural gas mixture (i.e., without hydrogen) ranges −0.58% to 0.41% above 0.1 Q_{max} and −0.65% to −0.19% below 0.1 Q_{max}. On the other hand, error of indication with 2E/H5 mixture ranges −0.68% to 0.26% above 0.1 Q_{max}, and 0.07% to 0.70% below 0.1 Q_{max}. The errors of indications of all gas meters with both the 2E/H0 and 2E/H5 mixtures, were within the permissible limits (i.e., ±2% in the range from 0.1 Q_{max} to Q_{max} and ±3.5% in the range below 0.1 Q_{max}) of EN 14236:2018 [23] for ultrasonic gas meters with temperature conversion. The maximum WME of the investigated gas meters was found: (i) ranging 0.01 % to 0.12 % for 2E/H0, (ii) ranging −0.22% to 0.00% for 2E/H5, and (iii) ranging −0.38 % to −0.10 % for

2E/H10 mixture. Table 7 shows the average error of indication drifts ($\Delta E_{2E\text{-}2E/H5}$) between 2E/H5 and 2E/H0 mixtures, together with the related metrological assessment.

Table 7. Metrological assessment of average error of indication drift of ultrasonic G4 gas meters with 2E/H5 and 2E/H0.

Flow Rate	Average Errors Drift [%]	Uncertainty in Average Errors [%]		Permitted Errors Difference [%]	Metrological Assessment
	$\Delta E_{m(2E\text{-}2E/H5)}$	$U(E_m)$ 2E/H5	2E	$U(\Delta E_{2E\text{-}2E/H5})$	
Q_{max}	−0.43	0.17	0.16	±0.46	insignificant
0.7 Q_{max}	−0.29	0.15	0.15	±0.42	insignificant
0.4 Q_{max}	−0.21	0.17	0.22	±0.55	insignificant
0.2 Q_{max}	−0.01	0.24	0.27	±0.72	insignificant
0.1 Q_{max}	0.35	0.21	0.14	±0.50	insignificant
3 Q_{min}	0.88	0.20	0.18	±0.53	significant
Q_{min}	0.71	0.28	0.24	±0.72	insignificant

In this case, the metrological assessment was found significant only at 3 Q_{min} flow rate, meaning that there is a slight influence on the gas meter accuracy when a 5% H2NG mixture is used. On the other hand, when analysing the errors of indications, it should be noted that hydrogen injection up to 10% vol. does not significantly affect the accuracy of gas meters.

4. Gas Quality Measurement of H2NG Mixtures

At present, typical process chromatographs dedicated to natural gas analyses do not allow the in-line determination of the hydrogen content. This is due to the fact that currently used process chromatographs (PGCs) use helium as a carrier gas, so they are not capable to detect and determine hydrogen due to the similar thermal conductivity of both these gases (151 and 180 $Wm^{-1}K^{-1}$ for helium and hydrogen, respectively). Therefore, solutions that can be used to analyze natural gas-hydrogen mixtures should be sought in devices dedicated to other types of gaseous fuels or constructed on the basis of customer guidelines. Aiming at analysing the composition of natural gas-hydrogen mixtures (hydrogen content up to 37% mol/mol), inter alia, a four-channel chromatograph equipped with four TCD detectors, can be used [25–27]. This device uses two carrier gases (argon and helium) and the declared duration of the analytical cycle for a configuration that allows determination of all required components is 3 to 5 min. A frequent calibration of this chromatograph is recommended ranging from daily to every 3 months.

On the other hand, in the refinery sector, a first solution relies on three-channel analysers that enable the determination of components in the gas such as hydrogen, helium, nitrogen, oxygen, carbon monoxide (II), carbon monoxide (IV) and hydrocarbons from the C1–C5 range, including unsaturated hydrocarbons broken down into isomers, and the total content of C6+ hydrocarbons [28,29]. These analysers are equipped with thermal conductivity detectors (TCD) and a flame ionization detector (FID), which is the third measurement channel enabling the determination of the content of hydrogen and other basic components of natural gas-hydrogen mixtures up to 100%. The typical time of analysis with their use is 15 min; however, it requires additional technical gases supplying the FID detector to the chromatograph, i.e., hydrogen and synthetic air as well as helium and nitrogen, which are reference gases in TCD detectors, which increases the cost of operating the device. Additionally, it is possible to reduce the analysis time to 7.5 min, if hydrogen is used as the carrier gas, then the hydrogen content in the sample is determined by using a TCD detector with nitrogen as the reference gas. However, due to the explosive properties of hydrogen, its use as a carrier gas in gas chromatography is often rejected by laboratories. Single (double) channel chromatograph with a single (double)

thermal conductivity detector (TCD) are also available [30,31], enabling in the scope of such components as pseudo-component C6+, hydrogen, helium, oxygen, carbon monoxide (IV), methane, ethane, propane, butanes, pentanes (with the double-channel configuration even nitrogen can be detected). Optionally the chromatograph can be equipped with an additional third channel with a flame ionization detector (FID), allowing individual determination of C6–C16 hydrocarbons. A further chromatograph dedicated to natural gas analyses enables the determination of the content of C1–C9 hydrocarbons, oxygen, nitrogen, carbon monoxide (IV), helium and hydrogen sulphide in the gas [32]. However, no detailed information on the range of the analysed concentrations and the duration of the analysis is available. An important feature of gas chromatographs dedicated to refinery gas analysis is that they allow the determination of hydrogen content in the entire concentration range by using two TCD detectors and an FID detector [33]. Depending on the model, the analysis time ranges from less than 9 min to 17 min.

Chromatographs for both H2NG mixtures and for refinery gas analyses are also available in the market [34,35]. Although chromatographs dedicated to refinery gas analyses are characterized by a sufficiently wide analytical range for hydrogen determination; however, due to the possibility of methane analysis only up to 80% mol/mol, they cannot be used in the case of analyses of certain mixtures of natural gas with hydrogen and natural gas from the H group. On the other hand, chromatographs dedicated to natural gas analyses allow for analysis in the scope of determination of at least: He, O_2, N_2, CH_4, CO, CO_2, C2–C5 hydrocarbons, H_2S and of course H_2 up to 10%. The analysis time depends on the model and ranges from 10 to 40 min. These chromatographs are equipped with two TCD detectors or two TCD detectors and a FID detector.

5. Conclusions

In this paper, the main thermophysical parameters of H2NG mixtures have been analysed as a function of the hydrogen (i.e., up to 25% vol.). The results obtained show that injection of H_2 into natural gas significantly impacts the relative density, specific heat and higher calorific value and speed of sound (which is a critical parameter for ultrasonic static gas meters), while the Wobbe Index is less affected. In particular:

- the relative density decreases as the H_2 content increases (e.g., for the investigated GAS 6 10%vol of H_2 is sufficient for the corresponding limit to be exceeded);
- the higher calorific value significantly decreases as the H_2 content increases (e.g., for gases characterized by a low content of CH_4, the calorific value is reduced by 20% when the hydrogen content is equal to 25%, exceeding the lower limit indicated by the ISO 12213-2 standard;
- the speed of sound increases up to 12.3% becoming generally higher than the accepted limit of 475 $m \cdot s^{-1}$ indicated by ISO 14236 for ultrasonic gas meters already at x_{H_2} = 5%.

The trend of the compressibility factor Z as a function of H_2 injection was also analysed using the available calculation algorithms of ISO 12213-2 (complete composition), ISO 12213-3, AGA NX 19 and AGA NX 19 Mod. The obtained results show that the compressibility factor at high pressures is more influenced by the presence of hydrogen than at low pressures (e.g., Z increases in the range 0.10–0.14% at 5 bar and in the range 2.1–9.1% at 70 bar). Moreover, the pressure influence on Z is more significantly impactful at low H_2 contents. A similar behaviour has been found for the volume conversion factor.

Finally, no influence on the deterioration of metrological properties was found for domestic G4 ultrasonic gas meters tested with the use of various gas mixtures with hydrogen content up to 10%. In fact, both the errors of indications and the weighted mean errors remained within the permissible limits, with measured errors not exceeding $\pm$1% and WME within $\pm$0.4%.

Author Contributions: Study conception and design: M.D., G.F., J.J. Acquisition, analysis and interpretation of data: All authors; Drafting of manuscript: L.M., G.F., P.K.; Critical revision: M.D., G.F., L.M., J.J., P.K., E.K.−Z. All authors have read and agreed to the published version of the manuscript and author contributions.

Funding: This research was funded by Regione Lazio, Progetti Strategici 2019 Progetto SINBIO "Sistemi INtegrati di produzione e immissione in rete di BIOmetano e gas sintetici da fonti rinnovabili," Grant number F82I20000300002.

Institutional Review Board Statement: Not applicable.

Informed Consent Statement: Not applicable.

Conflicts of Interest: The authors declare no conflict of interest.

Glossary

Nomenclature

c_p	specific heat capacity, [kJ/(kg·K)];
D	mass density, [kg/m^3];
D_t	diameter of the measurement tube, [m];
G	relative density, dimensionless;
Hv	higher heating value on volume basis, [MJ/m^3];
k	adiabatic coefficient, dimensionless;
$KTvo$	volumetric correction factor, dimensionless;
L	distance between the ultrasonic transducers, [m];
M	molar mass, [kg/kmol];
p	gas pressure, [bar];
Q	flow rate, [m^3/h];
R	universal gas constant, [MJ/(kmol·K)]
t	Celsius temperature, [°C];
t_i	transit time, [sec];
T	absolute temperature, [K];
u	speed of sound, [m/s];
V	volume, [m^3];
W	Wobbe Index, [MJ/m^3];
$\overline{w}$	average velocity of the gas flow, [m/s];
x	molar fraction, dimensionless;
Z	compressibility factor, dimensionless;
ρ_m	molar density, [kmol/m^3];
ρ_r	reduced density of gas, dimensionless;
φ	propagation angle, [°];
MPE	maximum permissible error, [%];
WME	weighted mean error, [%];
E	error of indications of the gas meters, [%];
E_m	average error of indications of the gas meters, [%];
E_{mAIR}	average error of indications of the gas meters using air, [%];
$U(E_m)$	uncertainty of the average error of indications, [%];

Abbreviations

INiG-PIB	Oil and Gas Institute–National Research Institute;
2E	natural gas of "E" group of EN 437:2019, second gas family (high methane);
2E/H0	2E natural gas mixture without hydrogen;
2E/H5	2E natural gas mixture with 5% hydrogen content [V/V];
2E/H10	2E natural gas mixture with 10% hydrogen content [V/V];

References

1. European Commission. *A Hydrogen Strategy for a Climate-Neutral Europe COM*; 301 Final; European Commission: Brussels, Belgium, 2020.
2. Perna, A.; Moretti, L.; Ficco, G.; Spazzafumo, G.; Canale, L.; Dell'Isola, M. SNG Generation via Power to Gas Technology: Plant Design and Annual Performance Assessment. *Appl. Sci.* **2020**, *10*, 8443. [CrossRef]
3. Tsai, Y.T.; Fu, T.; Zhou, Q. Explosion characteristics and suppression of hybrid Mg/H_2 mixtures. *Int. J. Hydrogen Energy* **2021**, *46*, 38934–38943. [CrossRef]
4. Tsai, Y.T.; Huang, G.T.; Zhao, J.Q.; Shu, C.M. Dust cloud explosion characteristics and mechanisms in MgH_2-based hydrogen storage materials. *AIChE J.* **2021**, *67*, e17302. [CrossRef]
5. Labidine Messaoudani, Z.; Rigas, F.; Binti Hamid, M.D.; Che Hassan, C.R. Hazards, Safety and Knowledge Gaps on Hydrogen Transmission via Natural Gas Grid: A Critical Review. *Int. J. Hydrogen Energy* **2016**, *41*, 17511–17525. [CrossRef]
6. Witkowski, A.; Rusin, A.; Majkut, M.; Stolecka, K. Analysis of Compression and Transport of the Methane/Hydrogen Mixture in Existing Natural Gas Pipelines. *Int. J. Press. Vessel. Pip.* **2018**, *166*, 24–34. [CrossRef]
7. Stetsenko, A.A.; Nedzelsky, S.D.; Naumenko, V.A. The Effect of Hydrogen on the Physical Properties of Natural Gas and the Metrological Characteristics of Its Metering Systems. *Metrol. Instrum.* **2020**, *6*, 45–50. [CrossRef]
8. Müller-Syring, G.; Henel, M.; Köppel, W.; Mlaker, H.; Sterner, M.; Höcher, T. *Entwicklung von Modularen Konzepten Zur Erzeugung, Speicherung und Einspeisung von Wasserstoff und Methan in Erdgasnetz*; DVGW (Hg.): Bonn, Germany, 2013.
9. Iskov, H.; Jensen, J. Field Test of Hydrogen in the Natural Gas Grid. In Proceedings of the 23rd World Gas Conference, Amsterdam, The Netherlands, 5–9 June 2006; Available online: https://www.dgc.dk/sites/default/files/filer/publikationer/C0605_field_test_hydrogen.pdf (accessed on 15 October 2021).
10. Dehaeseleer, J. The Effects of Injecting Hydrogen (Renewable Gases). In Proceedings of the EASEE-Gas GMOM, Budapest, Hungary, 28 March 2018.
11. Jaworski, J.; Kułaga, P.; Blacharski, T. Study of the Effect of Addition of Hydrogen to Natural Gas on Diaphragm Gas Meters. *Energies* **2020**, *13*, 3006. [CrossRef]
12. Jaworski, J.; Dudek, A. Study of the Effects of Changes in Gas Composition as Well as Ambient and Gas Temperature on Errors of Indications of Thermal Gas Meters. *Energies* **2020**, *13*, 5428. [CrossRef]
13. MARCOGAZ. *Overview of Test Results and Regulatory Limits for Hydrogen Admission into Existing Natural Gas Infrastructure and End Use 2019*; MARCOGAZ: Brussels, Belgium, 2019; Available online: https://www.marcogaz.org/wp-content/uploads/2019/09/H2-Infographic.pdf (accessed on 15 October 2021).
14. Łach, M. Dokładność Wyznaczania Współczynnika Ściśliwości Gazu z Podwyższoną Zawartością Wodoru—Porównanie Metod Obliczeniowych. *NG* **2016**, *72*, 329–338. [CrossRef]
15. ISO. *UNI EN ISO 6976:2017 Natural Gas—Calculation of Calorific Values, Density, Relative Density and Wobbe Indices from Composition*; ISO: Geneva, Switzerland, 2017.
16. Coker, A.K.; Ludwig, E.E. *Ludwig's Applied Process Design for Chemical and Petrochemical Plants*, 4th ed.; Elsevier Gulf Professional Pub: Amsterdam, The Netherlands; Boston, MA, USA, 2007; ISBN 978-0-7506-7766-0.
17. American Gas Association. *Speed of Sound in Natural Gas and Other Related Hydrocarbon Gases*; AGA REPORT #10; American Gas Association: Washington, DC, USA, 2003.
18. ISO. *UNI EN ISO 12213-2:2010 Natural Gas—Calculation of Compression Factor Calculation Using Molar-Composition Analysis*; ISO: Geneva, Switzerland, 2010.
19. Jaeschke, M.; Humphreys, A.E. *Standard GERG Virial Equation for Field Use: Simplification of the Input Data Requirements for the GERG Virial Equation: An Alternative Means of Compressibility Factor Calculation for Natural Gases and Similar Mixtures*; Fortschrittberichte VDI Reihe 6, Energietechnik; VDI-Verl: Düsseldorf, Germany, 1992; ISBN 978-3-18-146606-3.
20. Farzaneh-Gord, M.; Mohseni-Gharyehsafa, B.; Toikka, A.; Zvereva, I. Sensitivity of Natural Gas Flow Measurement to AGA8 or GERG2008 Equation of State Utilization. *J. Nat. Gas Sci. Eng.* **2018**, *57*, 305–321. [CrossRef]
21. Ficco, G.; Celenza, L.; Dell'Isola, M.; Vigo, P. Experimental evaluation of thermal mass smart meters influence factors. *J. Nat. Gas Sci. Eng.* **2016**, *32*, 1–10. [CrossRef]
22. Network Code. *Annex 11/A, Network Code—Upgrade LXIV*; SNAM Rete Gas: Milan, Italy, 2019; Available online: https://www.snam.it/export/sites/snam-rp/repository-srg/file/en/business-services/network-code-tariffs/Network_Code/Codice_di_Rete/64.CdR_LXIV/64.SRG_Network_Code_Rev_LXIV_ENG.pdf (accessed on 15 October 2021).
23. CEN. *BS EN 14236:2018 Ultrasonic Domestic Gas Meters*; CEN: Brussels, Belgium, 2018.
24. International Organization of Legal Metrology. OIML R 137—1 & 2 International Recommendation. Gas Meters. Part 1 and Part 2. 2012. Available online: https://www.oiml.org/en/files/pdf_r/r137-1-2-e12.pdf (accessed on 20 October 2021).
25. Available online: https://www.inficon.com/en/products/micro-gc-fusion-gas-analyzer (accessed on 15 October 2021).
26. Available online: https://www.intergaz.eu/produkty/analiza-jakosci-gazu/analizatory/chromatograf-encal-3000/ (accessed on 15 October 2021).
27. Available online: https://envag.com.pl/produkty/chromatografy-przemyslowe/chromatografy/przemyslowy-modulowy-chromatograf-gazowy-maxum-edycja-ii/ (accessed on 15 October 2021).
28. Available online: https://www.perkinelmer.com/pl/product/arnel-model-1115ppc590-narl8105 (accessed on 15 October 2021).

29. Available online: https://www.perkinelmer.com/pl/product/rga-column-set-with-h2-channel-n6107033 (accessed on 15 October 2021).
30. Available online: https://tools.thermofisher.com/content/sfs/brochures/BR-10484-Natural-Gas-Analyzers-BR10484-EN.pdf (accessed on 15 October 2021).
31. Available online: https://www.thermofisher.com/order/catalog/product/NATGASC20211?SID=srch-srp-NATGASC20211 (accessed on 15 October 2021).
32. Available online: https://www.agilent.com/cs/library/applications/5991-0275EN.pdf (accessed on 15 October 2021).
33. Available online: https://www.agilent.com/cs/library/brochures/5991-4156EN_LR.pdf (accessed on 15 October 2021).
34. Available online: https://www.shimadzu.com/an/system-gc/n9j25k00000fndbr.html (accessed on 15 October 2021).
35. Available online: https://www.shimadzu.com/an/products/gas-chromatography/application-specific-system-gc/natural-gas-analysis/index.html (accessed on 15 October 2021).